Supporting information for

Reduced $Na_{2+x}Ti_4O_9$/C composite: a durable anode for sodium-ion batteries

Dries De Sloovere,[a,b] Mohammadhosein Safari,[a,b] Ken Elen,[a,c] Jan D'Haen,[a] Oleg A. Drozhzhin,[d,e] Artem M. Abakumov,[d] Mantas Šimėnas,[f] Juras Banys,[f] Jonas Bekaert,[g] Bart Partoens,[g] Marlies K. Van Bael,[a,b] An Hardy[a,b]

[a]UHasselt, Institute for Materials Research (IMO-imomec), Martelarenlaan 42, B-3500 Hasselt, Belgium

[b]Energyville, Thor Park 8320, B-3600 Genk, Belgium

[c]IMEC vzw, Division Imomec, Wetenschapspark 1, B-3590 Diepenbeek, Belgium

[d]Center for Electrochemical Energy Storage, Skolkovo Institute of Science and Technology, Nobel Str. 3, 143026 Moscow, Russia

[e]Chemistry Department, Lomonosov Moscow State University, Leninskie gory 1, Moscow 119991, Russian Federation

[f]Faculty of Physics, Vilnius University, Sauletekio 9, 10222 Vilnius, Lithuania

[g]Condensed Matter Theory Group, Department of Physics, University of Antwerp, Groenenborgerlaan 171, 2020 Antwerpen, Belgium

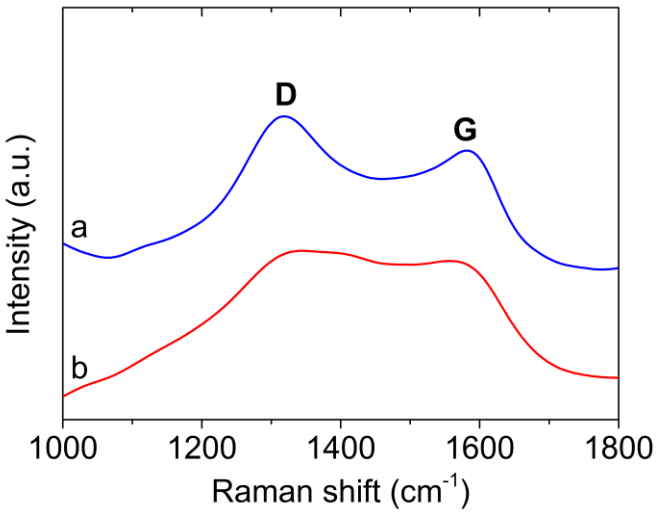

Figure S1: Experimental Raman spectra of $Na_{2+x}Ti_4O_9$/C (a), and of amorphous carbon (b).

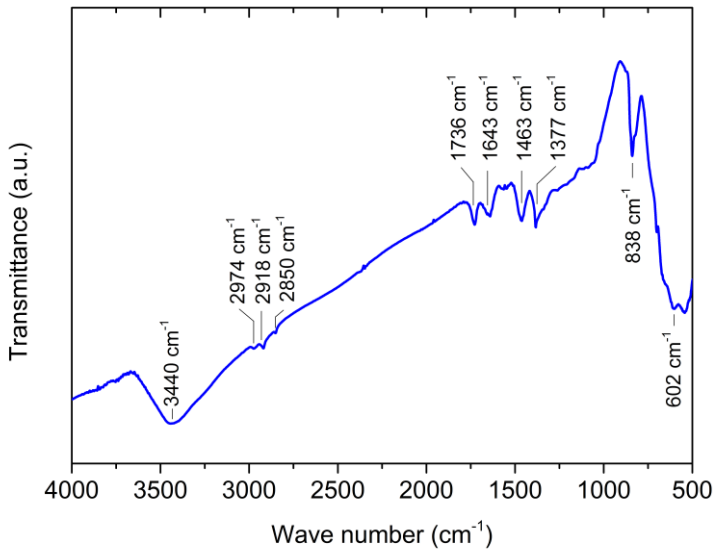

Figure S2: FTIR spectrum of $Na_{2+x}Ti_4O_9$/C.

Table S1: Assignment of the peaks in Figure S2.

Wave number (cm^{-1})	Vibration assignment
3440	ν_s(O-H) H_2O
2974	ν_s(C-H)
2918	ν_s(C-H)
2855	ν_s(C-H)
1736	ν_s(C=O)
1643	ν_s(C=O) amide
1463	ν_s(C-N) amide
1377	ν_b(C-O)
838	ν_b(C-H)
602	ν_s(Ti-O)

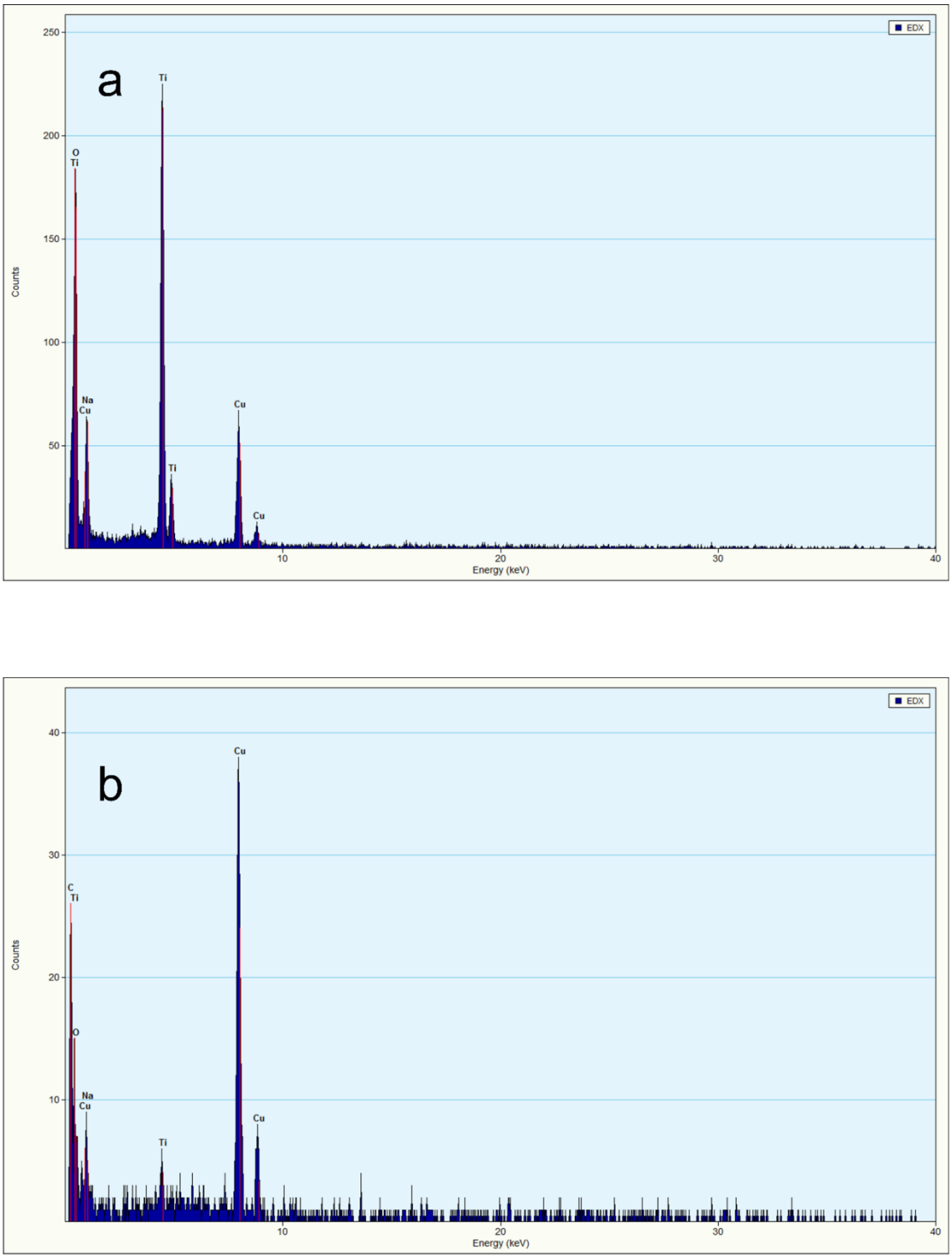

Figure S3: EDX of (a) a rod-shaped particle and (b) irregular nanoparticles found in $Na_{2+x}Ti_4O_9$/C. The Cu signal originates from the specimen support.

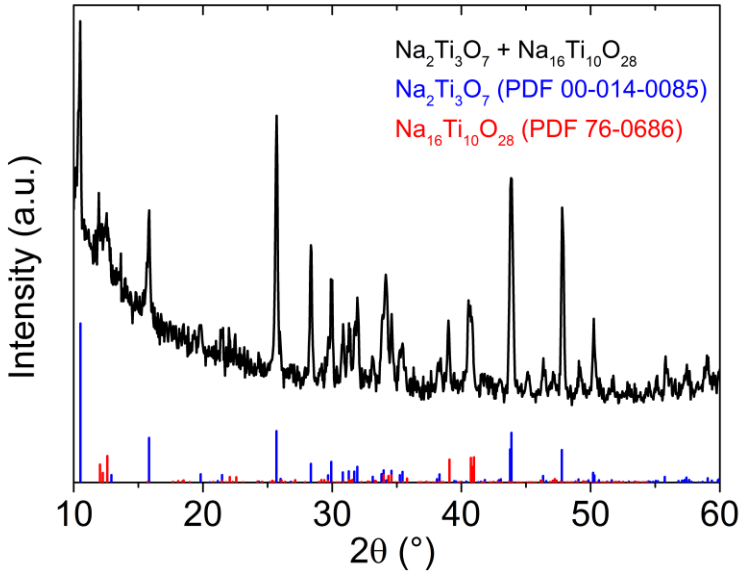

Figure S4: X-ray powder diffraction pattern of the Na^{+}-Ti^{4+} precursor thermally processed for 2 hours under air, and references.

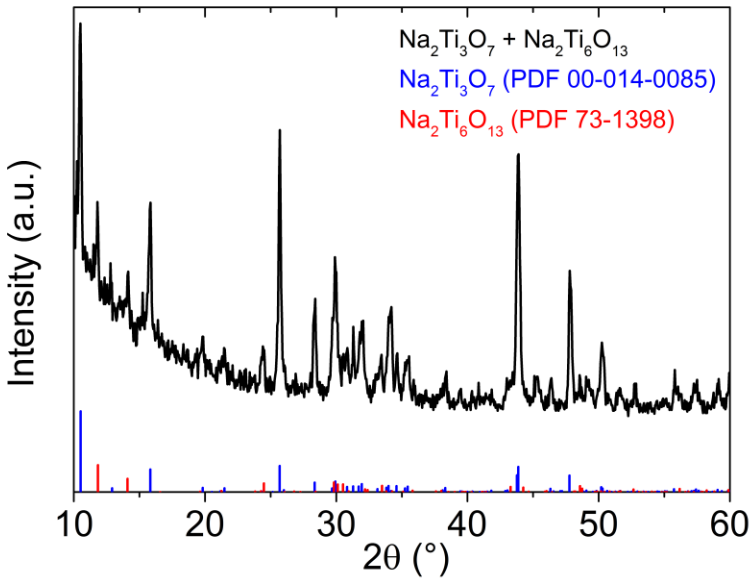

Figure S5: X-ray powder diffraction pattern of $Na_{2+x}Ti_4O_9$/C after thermal processing in air for 2 hours, and references.

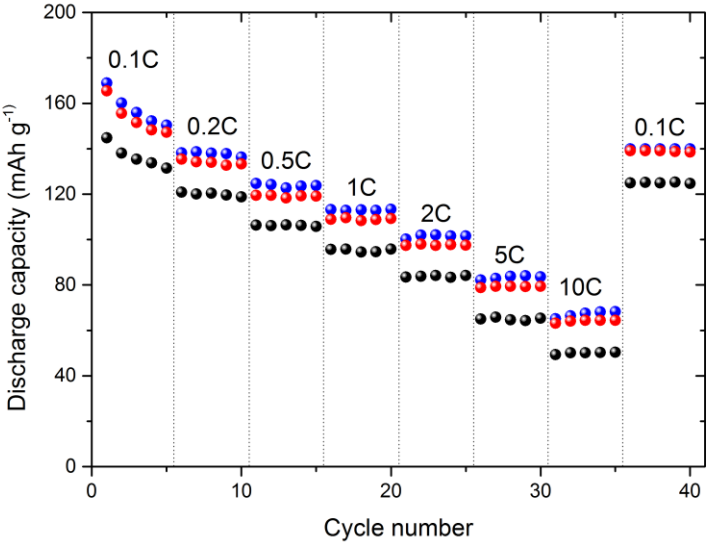

Figure S6: Individual discharge capacity measurements of $Na_{2+x}Ti_4O_9$ at rates from 0.1C to 10C.

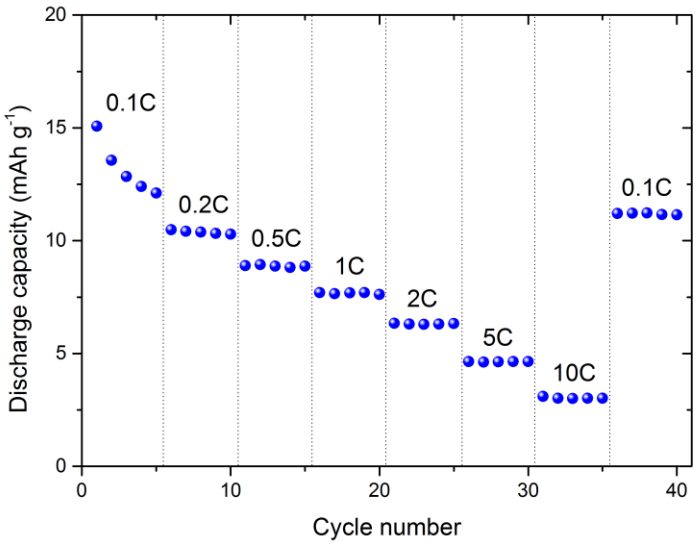

Figure S7: Discharge capacity of carbon black at rates from 0.1C to 10C. Whereas the slurries for these batteries contained only the additive carbon black and PVDF, the C-rates indicated in the graph are calculated according to a loading of 2.55 mg cm^{-2} $Na_{2+x}Ti_4O_9$/C. This makes it possible to determine the capacity contribution of carbon black at every C-rate.

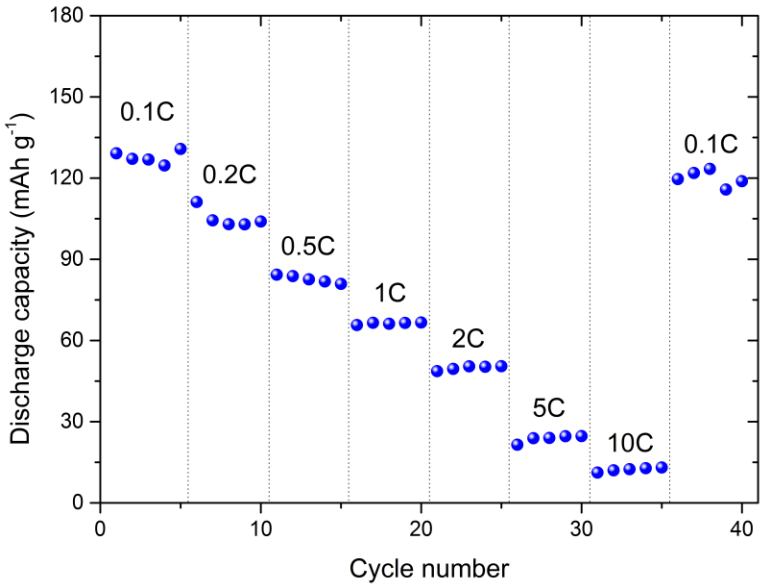

Figure S8: Discharge capacity of amorphous carbon at rates from 0.1C to 10C.

Density functional theory calculations Density functional theory (DFT) calculations on both $Na_3Ti_4O_9$ (64 atoms per unit cell) and $Na_2Ti_4O_9$ (60 atoms per unit cell), where the latter was characterized by introducing one Na vacancy per formula unit, were performed making use of the generalized gradient approximation (GGA), specifically of the Perdew-Burke-Ernzerhof (PBE) functional, implemented within a plane wave basis in the ABINIT code.[47] Electron-ion interactions were treated using norm-conserving pseudopotentials,[48] taking into account Na $2s^2 2p^6 3s^1$, Ti $3s^2 3p^6 3d^2 4s^2$ and O $2s^2 2p^4$ as valence electrons. The energy cutoff for the plane-wave basis was set to 40 Ha, to achieve convergence of the total energy below 1 meV per atom. The k-point grid used for integration over the Brillouin zone measured 2x15x4. The notational convention established by Setyawan and Curtarolo (2010)[49] was used to denote the high-symmetry k-points. The crystal structure relaxation was performed using a conjugate-gradient algorithm ensuring that forces on each atom were below 1 meV $Å^{-1}$.

The stoichiometric composition of $Na_{2+x}Ti_4O_9$ is $Na_3Ti_4O_9$, with one titanium ion in the 3+ oxidation state. In the calculated band structure of $Na_3Ti_4O_9$ (Figure S8a), the band at the Fermi level suggests a metal-like

behavior. Because of the gap between this band and the underlying band, $Na_3Ti_4O_9$ is energetically unfavorable. By randomly creating Na^+ vacancies, and thereby obtaining $Na_2Ti_4O_9$, the Fermi level is lowered and the material becomes an indirect semiconductor with a valence band maximum between Γ and Y and a conduction band minimum between X and X1 (Figure S8b). The band gap is found to amount to 2.2 eV. Due to the use of the semi-local PBE functional in the calculation, this gap may be underestimated.[50] Nevertheless, it is clear that this compound is not conductive.

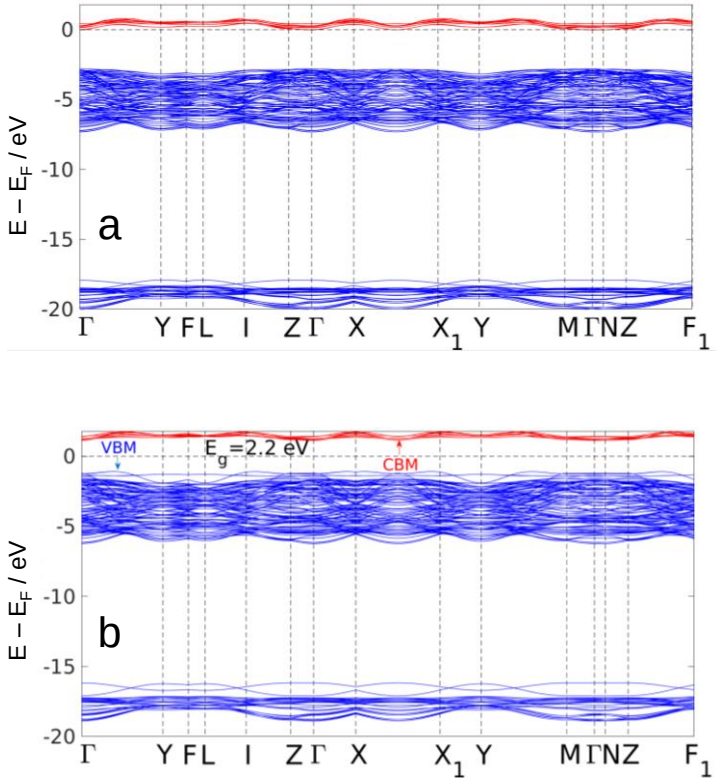

Figure S9: The calculated band structure along points of high symmetry in the irreducible Brillouin zone of stoichiometric $Na_3Ti_4O_9$ (a) and $Na_2Ti_4O_9$ (b). Valence bands are depicted as blue and conduction bands as red.

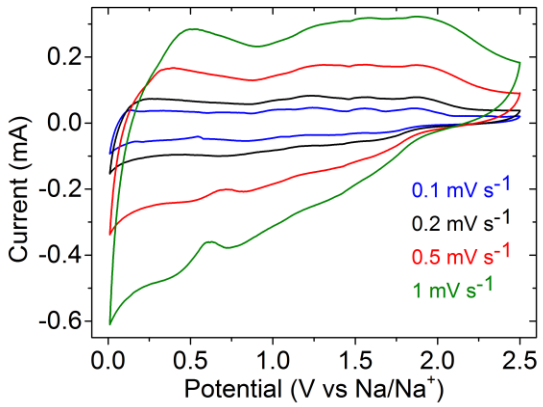

Figure S10: CV of a $Na_{2+x}Ti_4O_9$/C – Na cell at 0.1 mV s^{-1}, 0.2 mV s^{-1}, 0.5 mV s^{-1} and 1 mV s^{-1}.

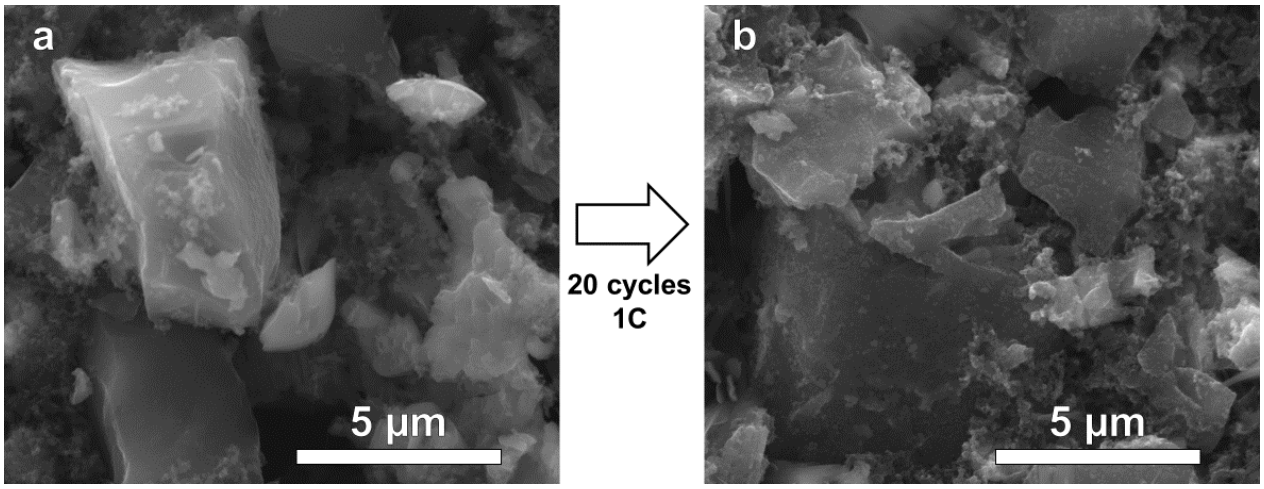

Figure S11: SEM images of $Na_{2+x}Ti_4O_9$/C electrodes: pristine (a) and after 20 charge/discharge cycles at 1C (b).

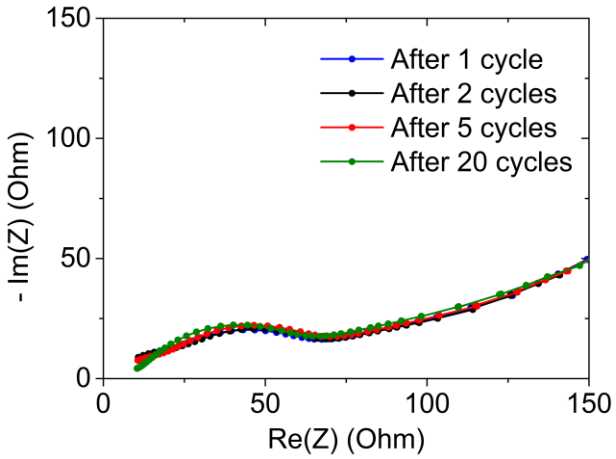

Figure S12: Nyquist plot representation of impedance spectra of $Na_{2+x}Ti_4O_9$/C – Na cells after 1, 2, 5 and 20 cycles at 1C (with an open circuit potential period of 2 hours after every cycle). The impedance spectra were recorded over a frequency range of 10 kHz to 10 mHz and subject to a potential amplitude of 10 mV.

References

(47) Gonze, X.; Amadon, B.; Anglade, P. M.; Beuken, J. M.; Bottin, F.; Boulanger, P.; Bruneval, F.; Caliste, D.; Caracas, R.; Côté, M.; et al. ABINIT: First-Principles Approach to Material and Nanosystem Properties. *Comput. Phys. Commun.* **2009**, *180* (12), 2582–2615.

(48) Hamann, D. R. Optimized Norm-Conserving Vanderbilt Pseudopotentials. *Phys. Rev. B - Condens. Matter Mater. Phys.* **2013**, *88* (8), 1–21.

(49) Setyawan, W.; Curtarolo, S. High-Throughput Electronic Band Structure Calculations: Challenges and Tools. *Comput. Mater. Sci.* **2010**, *54* (2), 299–312.

(50) Aulbur, W. G.; Jönsson, L.; Wilkins, J. W. Quasiparticle Calculations in Solids. *Solid State Phys.* **1999**, *54*, 1–218.